

# On the Photochemical Behavior of the $[\text{Ru}(\text{NH}_3)_4(\text{NO})\text{nicotinamide}]^{3+}$ Cation and the Relative Stability of Light-Induced Metastable Isonitrosyl Isomers of Ru Complexes

Christopher Kim,<sup>†</sup> Irina Novozhilova,<sup>†</sup> M. Scott Goodman,<sup>‡</sup> Kimberly A. Bagley,<sup>‡</sup> and Philip Coppens<sup>\*,†</sup>

Departments of Chemistry, State University of New York at Buffalo, Buffalo, New York 14260-300, and State University College of New York at Buffalo, Buffalo, New York, 14222

Received May 31, 2000

Low-temperature IR experiments on crystalline samples of *trans*- $[\text{Ru}(\text{NH}_3)_4(\text{NO})\text{nicotinamide}]^{3+}$  salts show a light-induced absorption band typical for MS1 NO linkage isomers upon exposure to 300–500 nm light from a Xe source. The formation of a metastable species is confirmed by DSC measurement on a sample irradiated at low temperature with 457 nm light from an Ar<sup>+</sup> laser. The light-induced species decays between 250 and 260 K according to both IR and DSC results. This decay temperature ( $T_d$ ) is somewhat below that observed for other high- $T_d$  linkage isomers, even though the NO-stretching frequency of the of  $[\text{Ru}(\text{NH}_3)_4(\text{NO})\text{nicotinamide}]^{3+}$  ion is above that of the other isomers, demonstrating a lack of precise correlation between the two physical properties. The 90 K crystal structure of *trans*- $[\text{Ru}(\text{NH}_3)_4(\text{NO})\text{nicotinamide}](\text{SiF}_6)(\text{NO}_3)\cdot\text{H}_2\text{O}$  is reported. The geometry from theoretical DFT calculations of the ground-state structure agrees well with the experimental results, except for the orientation of the CONH<sub>2</sub> substituent in the pyridine ring, which is rotated by 180° in the crystal due to packing effects. The MS1 and MS2 linkage isomers are found to correspond to local minima on the ground-state potential energy surface, and their geometries and energies are reported.

## Introduction

Recent crystallographic and theoretical results indicate that the photoinduced states of transition metal nitrosyl complexes, which were initially discovered in 1977 by Mössbauer and IR techniques,<sup>1,2</sup> are linkage isomers rather than long-lived electronically excited states. In the isomers, the nitrosyl group is bound through the oxygen atom (isonitrosyl, MS<sub>1</sub>) or through both oxygen and nitrogen in a bidentate side-on arrangement ( $\eta^2$ , MS<sub>2</sub>).<sup>3,4</sup> The ligand rearrangements are not limited to inorganic coordination compounds, but also occur upon 400–500 nm irradiation of metalloorganic complexes such as  $[\text{Ni}(\text{NO})(\eta^5\text{-Cp})]$  (Cp = cyclopentadienide<sup>5</sup> or pentamethylcyclopentadienide<sup>6</sup>) and for the biologically relevant six-coordinate Ru nitrosyl<sup>7</sup> and five- and six-coordinate Fe porphyrins.<sup>8</sup> A side-bound bidentate *dinitrogen* complex is formed upon irradiation of an Os complex with light of 325 nm wavelength.<sup>9</sup>

Thus, the light-induced formation of linkage isomers of oligoatomic ligands may be a more general phenomenon than previously recognized.

The light-induced species are metastable, but in many cases have practically infinite lifetimes when kept below liquid nitrogen temperature. The effect is reversible, as the ground-state conformation is recovered on subsequent warming or bleaching by irradiation of light of a longer wavelength. The temperature at which the metastable state decays ( $T_d$ ) can be determined by several techniques, including differential scanning calorimetry (DSC) and temperature-dependent IR experiments on light-irradiated samples.

The large differences between  $T_d$  of different complexes that have been observed merit further examination. They are of potential applied interest, as information storage systems based on the NO linkage isomers have been proposed. The application is based on the change in refractive index of the irradiated part of the crystals, which can be erased by subsequent exposure to light of longer wavelength.<sup>10–12</sup> For such an application to be of practical importance, identification of room-temperature stable linkage isomers is essential.

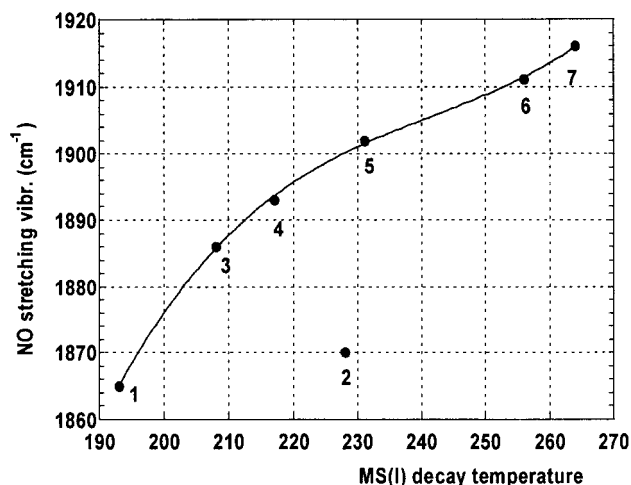
Different definitions of the decay temperature  $T_d$  occur in the literature. Frequently,  $T_d$  is defined as the minimum in the DSC curve obtained by monitoring the heat transfer, at a constant rate of increase in temperature, to a sample previously irradiated at low temperature. In the work of Morioka and collaborators, on the other hand, the decay temperature is defined

<sup>†</sup> State University of New York at Buffalo.

<sup>‡</sup> State University College of New York at Buffalo.

- (1) (a) Hauser, U.; Oestreich, V.; Rohrweck, H. D. *Z. Phys. A* **1977**, *280*, 17–25. (b) Hauser, U.; Oestreich, V.; Rohrweck, H. D. *Z. Phys. A* **1977**, *280*, 125–130.
- (2) Crichton, O.; Rest, A. *J. Chem. Soc., Dalton Trans.* **1977**, 986–993.
- (3) Coppens, P.; Fomitchev, D.; Carducci, M. D.; Culp, K. *J. Chem. Soc., Dalton Trans.* **1998**, 865–872.
- (4) Carducci, M. D.; Pressprich, M. R.; Coppens, P. *J. Am. Chem. Soc.* **1997**, *119*, 2669–2678.
- (5) (a) Chen, L. X.; Bowman, M. K.; Wang, Z.; Montano, P. A.; Norris, J. R. *J. Phys. Chem.* **1994**, *98*, 9457–9464. (b) Schaiquevich, P. S.; Guida, J. A.; Aymonio, P. J. *Inorg. Chim. Acta* **2000**, *303*, 277–281.
- (6) Fomitchev, D. V.; Furlani, T. R.; Coppens, P. *Inorg. Chem.* **1998**, *37*, 1519–1526.
- (7) Fomitchev, D. V.; Coppens, P.; Li, T.; Bagley, K. A.; Chen, L.; Richter-Addo, G. B. **1999** *Chem. Commun.* 2013–2014.
- (8) Cheng, L.; Novozhilova, I.; Kim, C.; Kovalevsky, A.; Bagley, K. A.; Coppens, P.; Richter-Addo, G. B. *J. Am. Chem. Soc.* **2000**, *122*, 7142–7143.

- (9) Fomitchev, D. V.; Bagley, K. A.; Coppens, P. *J. Am. Chem. Soc.* **2000**, *122*, 532–533.
- (10) Woike, Th.; Haussühl, B.; Sugg, B.; Rupp, R. A.; Beckers, J.; Imlau, M.; Schieder, R. *Physics B* **1996**, 243–248.
- (11) Woike, T.; Imlau, M.; Haussühl, S.; Rupp, R. A.; Schieder, R. *Phys. Rev. B* **1998**, *58* (13), 8411–8415.
- (12) Imlau, M.; Woike, T.; Schieder, R.; Rupp, R. A. *Phys. Rev. Lett.* **1999**, *82* (14), 2860–2863.



- 1 [Ru(NO)(bpy)(NO<sub>2</sub>)(OH)(H<sub>2</sub>O)][NO<sub>2</sub>]
- 2 [Ru(NO)(OH)(py)<sub>4</sub>][PF<sub>6</sub>]<sub>2</sub>
- 3 K<sub>2</sub>[Ru(NO)(NO<sub>2</sub>)<sub>4</sub>(OH)]
- 4 K<sub>2</sub>[Ru(NO)Cl<sub>4</sub>]
- 5 [Ru(NO)Br(py)<sub>4</sub>][PF<sub>6</sub>]<sub>2</sub>
- 6 [Ru(NO)Cl(py)<sub>4</sub>][PF<sub>6</sub>]<sub>2</sub>
- 7 [Ru(NO)(NH<sub>3</sub>)<sub>5</sub>][NO<sub>3</sub>]<sub>3</sub>

**Figure 1.** Decay temperature of MS1 for a number of complexes as a function of the ground-state NO-stretching frequency.

as the temperature at which the decay rate constant is 0.001 s<sup>-1</sup>. For sodium nitroprusside, Na<sub>2</sub>[Fe(CN)<sub>5</sub>NO] (SNP), the DSC decay temperatures are 195 K<sup>4</sup> to 200 K<sup>13</sup> for the isonitrosyl isomer MS1, and 151 K for the side-bound MS2, while Morioka et al. report an MS1 value of 182 K,<sup>14</sup> suggesting that the two definitions can lead to differences as large as 15°.

Since the initial discovery of the light-induced states of SNP, a considerable increase in  $T_d$  has been attained. For the NO<sub>3</sub><sup>-</sup> and PF<sub>6</sub><sup>-</sup> salts of [Ru(NH<sub>3</sub>)<sub>5</sub>(NO)]<sup>3+</sup> respectively, MS1-decay temperatures as high as 260 and 267 K, respectively, have been observed.<sup>15</sup> An MS1 decay temperature of 277 K for *trans*-[Ru(Hox)(en)<sub>2</sub>NO]Cl<sub>2</sub> (ox = oxalate, en = ethylenediamine) was reported recently by Morioka et al.<sup>14</sup>

The difference in  $T_d$  for the two salts of [Ru(NH<sub>3</sub>)<sub>5</sub>(NO)]<sup>3+</sup> illustrates that the crystalline environment has an effect on the stability of the metastable states. Nevertheless, variations occurring on chemical substitution are dominant, and should be explored in the search for high- $T_d$  linkage isomers.

#### The Relative Stability of the Isonitrosyl Linkage Isomers.

To test the *trans* influence<sup>16</sup> on the stability of the NO linkage isomers, we prepared, in previous work, a series of Ru complexes with different ligands in the position *trans* to NO. Though the equatorial ligands differ, the value of  $T_d$  tends to correlate with the NO-stretching frequency, as illustrated in Figure 1.

The complexes with the higher NO-stretching frequency are those with the strongest  $\pi$ -withdrawing *trans* ligand.<sup>17</sup> The electron-withdrawing power of the *trans* ligand is demonstrated by the redox potentials of a series of [Ru(NH<sub>3</sub>)<sub>4</sub>(NO)L]<sup>3+</sup>

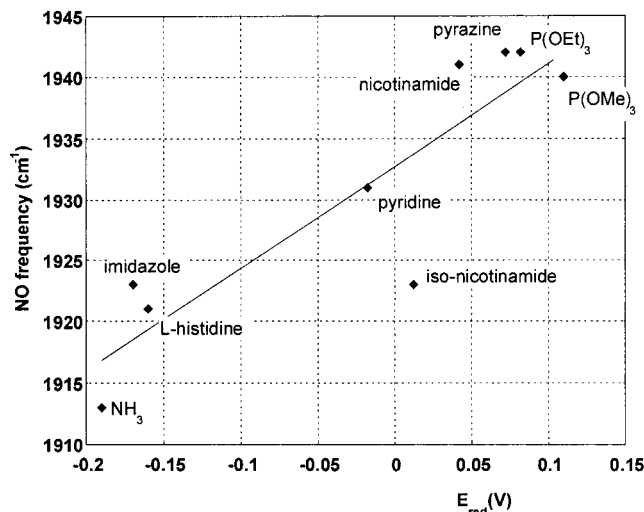


**Figure 2.** NO-stretching frequency vs redox potential for a number of *trans*-[Ru(NO)(NH<sub>3</sub>)<sub>4</sub>L] complexes. Data from ref 18.

complexes, reported by Lopes et al.,<sup>18</sup> with NO-stretching frequencies between 1910 and 1945 cm<sup>-1</sup> (Figure 2). Among the species examined in this study, the *trans*-nicotinamide ion, [Ru(NH<sub>3</sub>)<sub>4</sub>(NO)nic]<sup>3+</sup> (nic = nicotinamide), has one of the most positive redox potentials and one of the highest NO-stretching frequencies. We report here a study of the structure and photochemical behavior of this ion by both experimental and theoretical methods.

## Experimental Section

**Infrared Spectroscopy.** Infrared spectra were collected using a BioRad FTS 40A Fourier transform infrared spectrometer equipped with a variable-temperature (8–300 K) cryostat (APD Heli-Tran; model LT-3-110). Metastable states were formed via illumination with light from a 300 W xenon arc lamp passed through a 330–500 nm band-pass filter. Infrared difference spectra were calculated by subtracting the spectra of the ground-state species at the same temperature from the spectrum of the metastable state formed upon illumination. The resolution of the resultant difference spectra was 1 cm<sup>-1</sup>.

**Preparation of the Samples.** All solvents employed were freshly distilled before use. The compounds *trans*-[Ru(NH<sub>3</sub>)<sub>4</sub>(SO<sub>3</sub>H)<sub>2</sub>], *trans*-[Ru(NH<sub>3</sub>)<sub>4</sub>(SO<sub>2</sub>)Cl]Cl, and *trans*-[Ru(NH<sub>3</sub>)<sub>4</sub>(SO<sub>4</sub>)nic]Cl were synthesized from [Ru(NH<sub>3</sub>)<sub>5</sub>Cl]Cl<sub>2</sub> (Aldrich Chemical Co.), as described in the literature.<sup>19</sup>

***trans*-[Ru(NH<sub>3</sub>)<sub>4</sub>(NO)nic](SiF<sub>6</sub>)(BF<sub>4</sub>)·2H<sub>2</sub>O (1) and *trans*-[Ru(NH<sub>3</sub>)<sub>4</sub>(NO)nic](SiF<sub>6</sub>)(NO<sub>3</sub>)·H<sub>2</sub>O (2).** A modification of the published procedure<sup>20</sup> was employed. *trans*-[Ru(NH<sub>3</sub>)<sub>4</sub>(SO<sub>4</sub>)nic]Cl (100 mg, 0.24 mmol) was dissolved with stirring in H<sub>2</sub>O (5 mL). After degassing of the solution with argon for 10 min, trifluoroacetic acid (5  $\mu$ L) and Zn amalgam (100 mg) were added. The solution immediately turned to the orange-red color of *trans*-[Ru(NH<sub>3</sub>)<sub>4</sub>(H<sub>2</sub>O)nic]<sup>2+</sup>. After 5 min, the solution was transferred via cannula to a solution previously prepared from argon-degassed 5 M HBF<sub>4</sub> (2.0 mL) and NaNO<sub>2</sub> (100 mg, 1.45 mmol). The resulting pale orange solution was frozen in liquid N<sub>2</sub> and then allowed to warm in the refrigerator for 24 h under argon. The pale orange microcrystalline product (45 mg, 32%) was filtered, washed with ethanol, and dried under vacuum. IR spectra were similar to those reported in the literature.<sup>20</sup> Specifically, a pronounced band corresponding to the BF<sub>4</sub><sup>-</sup> ion was observed at  $\sim$ 1070 cm<sup>-1</sup>, while two overlapping peaks assigned to NO-stretching vibrations were observed (at 80 K) at

(13) Zöllner, H.; Woike, Th.; Krasser, W. *Z. Kristallogr.* **1989**, *188*, 139–153.

(14) Morioka, Y.; Ishikawa, A.; Tomizawa, H.; Miki, E.-I. *J. Chem. Soc., Dalton Trans.* **2000**, 781–786.

(15) Fomitchev, D. V.; Novozhilova, I.; Coppens, P. *Tetrahedron* **2000**, *56*, 6813–6820.

(16) Pidcock, A.; Richards, R. E.; Venanzi, L. M. *J. Chem. Soc. A* **1966**, 1707–1712.

(17) Cotton, F. A.; Wilkinson, G. *Advanced Inorganic Chemistry*; Wiley & Sons: New York, 1988.

(18) Lopes, L. G. F.; Gomes, M. G.; Borges, S. S. S.; Franco, D. W. *Aust. J. Chem.* **1998**, *51*, 865–866.

(19) (a) Vogt, L. H., Jr.; Katz, J. L.; Wiberley, S. E. *Inorg. Chem.* **1965**, *4*, 1157–1163. (b) Brown, G. M.; Sutton, J. E.; Taube, H. *J. Am. Chem. Soc.* **1978**, *100*, 2767–2774.

(20) Borges, S. S. S.; Davanzo, C. U.; Castellano, E. E.; Z-Schpector, J.; Silva, S. C.; Franco, D. W. *Inorg. Chem.* **1998**, *37*, 2670–2677.

**Table 1.** Crystallographic Data on *trans*-[Ru(NH<sub>3</sub>)<sub>4</sub>(NO)nic](SiF<sub>6</sub>)(NO<sub>3</sub>)·H<sub>2</sub>O

empirical formula	C <sub>6</sub> H <sub>20</sub> F <sub>6</sub> N <sub>8</sub> O <sub>6</sub> RuSi
fw	543.46
temp	90(1) K
wavelength	0.71073 Å
cryst syst	monoclinic
space group	<i>P</i> 2 <sub>1</sub> / <i>n</i>
unit cell dimens	<i>a</i> = 12.2636(6) Å <i>b</i> = 9.2147(4) Å <i>c</i> = 15.3394(7) Å $\alpha$ = 90° $\beta$ = 90.4970(10)° $\gamma$ = 90°
vol	1733.37(14) Å <sup>3</sup>
Z	4
density (calcd)	2.0825 Mg/m <sup>3</sup>
abs coeff	1.083 mm <sup>-1</sup>
cryst size	0.12 × 0.06 × 0.07 mm <sup>3</sup>
(sin $\theta/\lambda$ ) <sub>max</sub>	0.679 Å <sup>-1</sup>
index ranges	-15 < <i>h</i> < 15, -12 < <i>k</i> < 7, -19 < <i>l</i> < 18
reflns collected	9618
indep reflns	3789 [ <i>R</i> (int) = 0.0279] <sup>a</sup>
completeness to $\theta = 28.87^\circ$	83.1%
refinement meth	full-matrix least-squares on <i>F</i> <sup>2</sup>
no. of variables	334
goodness-of-fit on <i>F</i> <sup>2</sup>	1.007
final <i>R</i> indices [ <i>I</i> > 2 $\sigma$ ( <i>I</i> )]	<i>R</i> 1 = 0.0254, <i>wR</i> 2 = 0.0619 <sup>c</sup>
<i>R</i> indices (all data)	<i>R</i> 1 = 0.0289, <i>wR</i> 2 = 0.0638

<sup>a</sup> *R*(int) =  $\sum |F_o^2 - F_c^2(\text{mean})| / \sum F_o^2$ . <sup>b</sup> *R*1 =  $\sum ||F_o| - |F_c|| / \sum |F_o|$ .  
<sup>c</sup> *wR*2 =  $\{\sum [w(F_o^2 - F_c^2)^2] / \sum w(F_o^2)^2\}^{1/2}$ .

~1964 and ~1945 cm<sup>-1</sup>. Crystals were grown by slow cooling in a refrigerator of a 5 M HBF<sub>4</sub> aqueous solution ~0.05 M in the product. Crystal structure analysis confirmed the presence of the SiF<sub>6</sub><sup>2-</sup> ions, but the BF<sub>4</sub><sup>-</sup> ions were highly disordered. Combination of the measured density (1.98 Mg/m<sup>3</sup>) and the observed cell dimensions indicated the presence of two water molecules of crystallization per formula unit, in agreement with IR absorption in the 3500–3700 cm<sup>-1</sup> region. Because of the extensive disorder, persisting at low temperature, the material was recrystallized from a 1 M HNO<sub>3</sub> solution to give *trans*-[Ru(NH<sub>3</sub>)<sub>4</sub>(NO)nic](SiF<sub>6</sub>)(NO<sub>3</sub>)·H<sub>2</sub>O (**2**), the crystals of which have a well-ordered structure. In **2** the NO stretching shows a single peak at 1939 cm<sup>-1</sup>, while the BF<sub>4</sub><sup>-</sup> band is absent, as expected.

**X-ray structure Determination.** X-ray data on **2** were collected at 90 K using a Bruker SMART1000 CCD diffractometer installed at a rotating anode source (Mo K $\alpha$  radiation) and equipped with an Oxford Cryosystems nitrogen gas-flow apparatus. The data were collected by the rotation method with a 0.3° frame width and 10 s exposure time per frame. They were integrated, scaled, sorted, and averaged using the SAINT software package of programs.<sup>21</sup> Numerical absorption corrections were applied using XPREP ( $\mu = 1.083 \text{ mm}^{-1}$ ) in the SHELXTL suite of programs.<sup>22</sup> The structure was solved with SHELXS and refined with SHELXL. The crystals contain one molecule of water per formula unit. Crystallographic data are given in Table 1, while the contents of the asymmetric unit are shown in Figure 3.

**DSC Experiment.** The amount of heat released during thermally stimulated decay of the metastable states was measured by a Perkin-Elmer differential scanning calorimeter DSC7. A window installed in the calorimeter enclosure allows laser irradiation of the specimen at 110 K. Polycrystalline samples were cooled to 110 K and irradiated with  $\lambda = 457.9 \text{ nm}$  light from an Ar<sup>+</sup> laser with a power 50 mW/cm<sup>2</sup>. The energy flux needed to achieve the steady state was determined in a series of experiments with variable exposure time. Once the laser was switched off, the system was allowed to come to thermal equilibrium for 10 min. The specimen was then heated at a constant rate of 5 K/min, while the enthalpy supplied for the heating was being monitored.

(21) SAINT Software Reference Manual; Bruker AXS; Madison, WI, 1998.  
(22) Sheldrick, G. M. SHELXTL NT Version 5.10, Program for the Refinement of Crystal Structures; University of Göttingen: Göttingen, Germany, 1997.

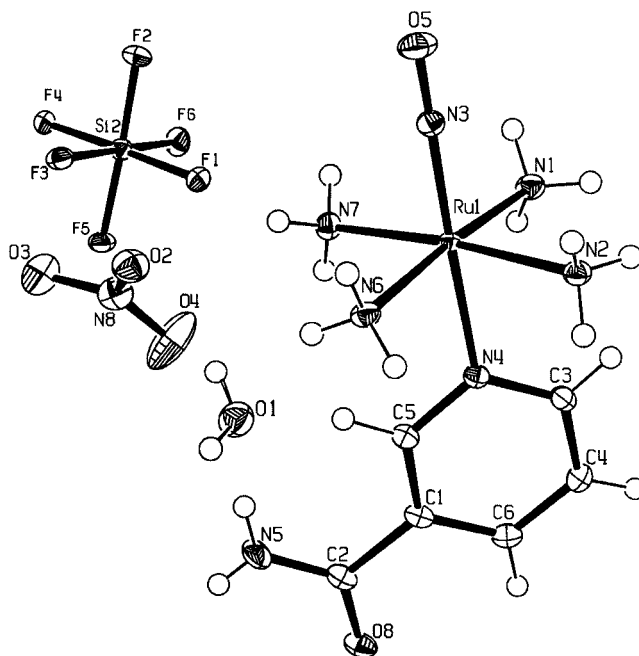


**Figure 3.** ORTEP plot of the asymmetric unit of *trans*-[Ru(NH<sub>3</sub>)<sub>4</sub>(NO)nic](SiF<sub>6</sub>)(NO<sub>3</sub>)·H<sub>2</sub>O at 90 K; 50% probability ellipsoids of the non-H atoms are shown.

**Theoretical Calculations.** All calculations were performed with the Amsterdam Density Functional (ADF) package.<sup>23</sup> For C, N, O, and halogen atoms, the valence shells were described using a triple- $\zeta$  STO basis set, augmented by one d-STO polarization function (ADF database IV). The atomic orbitals of hydrogen were described by a double- $\zeta$  basis set, augmented by one p-STO polarization function. For the *ns*, *np*, *nd*, (*n*+1)*s* and (*n*+1)*p* shells on Ru, a triple- $\zeta$  STO basis set was employed. The 1s<sup>2</sup> shell of C, N, O, 1s<sup>2</sup>2s<sup>2</sup>2p<sup>6</sup> of halogens, and the 1s<sup>2</sup>2s<sup>2</sup>2p<sup>6</sup>3s<sup>2</sup>3p<sup>6</sup>3d<sup>10</sup> shells of Ru were treated by the frozen-core approximation. Unless otherwise mentioned, calculations were based on the local density approximation (LDA) in the parametrization of Vosko, Wilk, and Nusair (VWN).<sup>24</sup> Scalar relativistic effects on Ru were taken into account with the Pauli formalism. In the geometry optimizations a convergence criterion for gradients of 10<sup>-3</sup> (au/Å) was used, while test integrals were evaluated with an accuracy of at least 8 significant digits.

All calculations were spin-restricted. The molecular geometries of the GS, MS1, and MS2 were fully optimized with no symmetry restrictions.

## Results and Discussion

**Crystal Structure.** In the crystals of **2** the CO(NH<sub>2</sub>) substituent is oriented with the oxygen atom pointing away from the Ru atom. Close examination of the reported room-temperature structure of [Ru(NH<sub>3</sub>)<sub>4</sub>(NO)nic]<sub>2</sub>(SiF<sub>6</sub>)<sub>3</sub>·2H<sub>2</sub>O<sup>20</sup> indicates that, of the four independent molecules in this structure, two have the previously reported configuration with the O atom toward Ru (the “cis” configuration), while the other molecules have the conformation observed for **2**. According to theory, the lowest energy state of the *isolated* molecule has the “cis”

(23) The Amsterdam Density Functional program package, v.1999.02; the Theoretical Chemistry group of the Vrije Universiteit in Amsterdam and the Theoretical Chemistry group of the University of Calgary, Canada. (a) Baerends, E. J.; Ellis, D. E.; Ros, P. *Chem. Phys.* **1973**, *2*, 41–51. (b) te Velde, G.; Baerends, E. J. *J. Comput. Phys.* **1992**, *99*, 84–98. (c) Fonseca Guerra, C.; Visser, O.; Snijders, J. G.; te Velde, G.; Baerends, E. J. In *Methods and Techniques for Computational Chemistry (METECC-5)*; Clementi, E., Corongiu, G., Eds.; STEF: Cagliari, 1995; pp 303–395.  
(24) Vosko, S. H.; Wilk, L.; Nusair, M. *Can. J. Phys.* **1980**, *58*, 1200–1211.



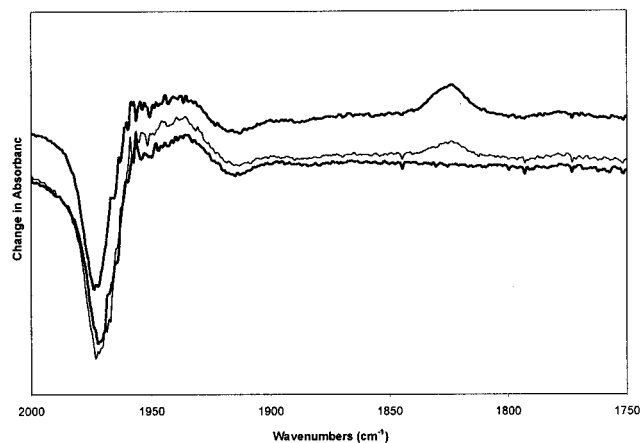


**Figure 4.** IR difference spectra after irradiation at 80 K and subsequent warming up to 250 K (top curve), 260 K (lighter middle curve), and 270 K (lower curve). Reference spectra for calculating the differences were obtained after warming up to room temperature and subsequent cooling. The disappearance of the light-induced band at  $\sim 1825\text{ cm}^{-1}$  on warming is evident. Curves are offset vertically to prevent overlap. Vertical scale in arbitrary units.

conformation. Optimization of the structure with the substituent constrained to be “trans” shows an energy increase relative to the completely optimized structure of 0.0225 H (59 kJ/mol), which in the crystal appears compensated for by more favorable intermolecular interactions. The atoms of the  $\text{CO}(\text{NH}_2)$  group participate in a number of hydrogen bonds with the water molecule of crystallization, the fluorine atoms, and the oxygen atoms of the nitrate ions.

**Observation of the Metastable Species.** Upon exposure of **1** at 80 K with 330–500 nm light (see above), the main NO-stretching band at  $1974\text{ cm}^{-1}$  and its shoulder at  $1918\text{ cm}^{-1}$  (frequencies at  $\sim 250\text{ K}$ ) disappear simultaneously, and a new band appears at  $1826\text{ cm}^{-1}$  as illustrated for the difference spectra shown in Figure 4. Upon illumination of **2**, a light-induced band is generated at  $1810\text{ cm}^{-1}$ , and a corresponding bleaching of the band centered at about  $1939\text{ cm}^{-1}$  is observed. The downshifts of  $148\text{--}92\text{ cm}^{-1}$  for **1** and  $129\text{ cm}^{-1}$  for **2** are similar to shifts observed for other Ru complexes, including ruthenium nitrosyl porphyrins ( $145\text{ cm}^{-1}$ ),<sup>7</sup> ethylenediamine-substituted Ru–NO complexes ( $125\text{--}134\text{ cm}^{-1}$ ),<sup>25</sup>  $\text{K}_2[\text{RuCl}_5(\text{NO})]$  ( $125\text{ cm}^{-1}$ ),<sup>26</sup> and  $\text{K}_2[\text{Ru}(\text{NO}_2)_4(\text{OH})(\text{NO})]$  ( $114\text{ cm}^{-1}$ ).<sup>27</sup> As in many of the other Ru complexes that have been investigated, no bands characteristic for MS2 were generated upon irradiation of either **1** or **2**. Examination of the temperature dependence of the difference spectra indicates a decay temperature between 250 and 260 K (Figure 4). DSC results on both **1** and **2** indicate a minimum centered at 256 K, in excellent agreement with the IR results.

Thus, the MS1 linkage isomer of the  $[\text{Ru}(\text{NH}_3)_4(\text{NO})\text{nic}]^{3+}$  ion is among the highest  $T_d$  isomers observed so far, but not as high as the isomers of the  $[\text{Ru}(\text{NH}_3)_5(\text{NO})]^{3+}$  and *trans*- $[\text{Ru}(\text{Hox})(\text{en})_2(\text{NO})]^{2+}$  species. As both the redox potential and the stretching frequency of  $[\text{Ru}(\text{NH}_3)_4(\text{NO})\text{nic}]^{3+}$  are higher than for the  $[\text{Ru}(\text{NH}_3)_5(\text{NO})]^{3+}$  ion, the correlation of these properties with  $T_d$  appears approximate at best.

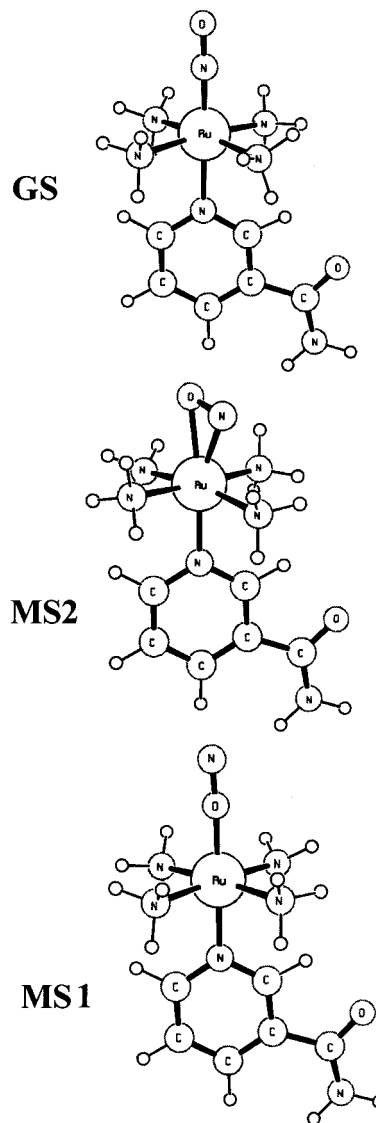


**Figure 5.** Theoretical conformations of the ground-state structure (GS) and the two linkage isomers.

**Theoretical Calculations. Ground and Metastable States of  $[\text{Ru}(\text{NH}_3)_4(\text{NO})\text{nic}]^{3+}$ .** The calculations indicate that both the MS1 and MS2 linkage isomers correspond to local minima on the potential energy surface. These observations were confirmed by following frequency calculations, which showed no negative eigenvalues in the Hessian matrices and no imaginary vibrations. For MS1 the energy is found to be 0.0658 H (1.79 eV) above that of the ground state, which may be compared with theoretical values of 1.746 eV, and 1.59 eV for SNP and FeP(NO) (P = porphine),<sup>8</sup> respectively. The calorimetrically determined value for SNP is 1.1 eV, suggesting that the  $\Delta E$  values are overestimated by the calculations. The energy for MS2 is found to be 1.54 eV above that of the ground state, which is slightly lower than for MS1, in accordance with both experimental<sup>13,28</sup> and theoretical results for other complexes.

The theoretical geometries for the ground state (GS) and the linkage isomers are shown in Figure 5. Numerical details are given in Table 2. The ground-state geometry is very well reproduced by the calculation. For MS1, the calculation predicts that the bond from Ru to the proximal atom of the NO group

(25) Ookubo, K.; Morioka, Y.; Tomizawa, H.; Miki, E. *J. Mol. Struct.* **1996**, *379*, 241–247.

(26) Woike, Th.; Zöllner, H.; Krasser, W.; Haussuhl, S. *Solid State Commun.* **1990**, *73*, 149–152.

(27) (a) Woike, Th.; Haussuhl, S. *Solid State Commun.* **1993**, *86*, 333–337. (b) Fomitchev, D. V.; Coppens, P. *Inorg. Chem.* **1996**, *35*, 7021–7026.

(28) Woike, Th.; Krasser, W.; Zöllner, H.; Kirchner, W.; Haussuhl, S. *J. Phys. D* **1993**, *25*, 351–356.

**Table 2.** Selected Theoretical Bond Lengths (Å) and Angles (deg) for the *trans*-[Ru(NH<sub>3</sub>)<sub>4</sub>(NO)nic]<sup>3+</sup> Ion

	exptl GS	GS	MS1	MS2
Ru–NO	1.752	1.775		1.960
Ru–ON			1.876	2.124
Ru–N(eq)	2.093	2.121	2.119	2.118
	2.107	2.119	2.121	2.135
	2.114	2.119	2.119	2.124
	2.118	2.120	2.117	2.118
Ru–N(trans)	2.124	2.077	2.024	2.044
N–O	1.136	1.137	1.142	1.186
∠RuNO, deg	178.7	179.37	179.64	80.86

**Table 3.** Selected Theoretical Results for [*trans*-LRu(NH<sub>3</sub>)<sub>4</sub>(NO)] Ions with Variable L<sup>a</sup>

L	OH <sup>-</sup>	Cl <sup>-</sup>	NO <sub>2</sub> <sup>-</sup>	H <sub>2</sub> O	nicotinamide	NH <sub>3</sub>
<i>d</i> <sub>NO</sub>	1.148	1.146	1.141	1.134	1.137	1.134
		1.142		1.144	1.136	1.139
<i>v</i> <sub>NO</sub>	1955.7	1962.4	1979.1	2028.5	2001.2	2022.7
π(NO)	0.0587	0.0658	0.0739	0.0747	0.0809	0.0839
∠N(O)RuN	95.6	94.8	97.2	93.4	93.3	92.6
		92.1		93.7		93.1
ΔE(MS1) (eV)	1.945	1.918	1.803	1.948	1.790	1.822

<sup>a</sup> Dimensions: bond lengths in Å; angles in deg; populations in e; energies in eV. Experimental values, when available, are given in the second row of each entry.

is lengthened, in agreement with crystallographic results on MS1 of other complexes, while the bond from Ru to the nitrogen atom trans to NO is shortened. The NO bond length increases somewhat upon isomerization (from 1.137 to 1.142 Å), in accordance with the decrease in NO-stretching frequency.

**Effect of Trans Substitution.** To analyze the trans influence, a series of calculations was performed with the same equatorial ligand, but varying trans substituents. The geometry was optimized in all cases. Selected results are summarized in Table 3, in which the high-*T*<sub>d</sub> *trans*-nic and *trans*-NH<sub>3</sub> complexes are listed on the right. The calculated NO-stretching frequencies tend to increase toward the right of the table, in conjunction with the π-NO overlap population *P*<sub>NO</sub>, defined as  $P_{NO} = \sum_{\mu\nu} P_{\mu\nu} S_{\mu\nu}$  where the sum is over all π-orbitals on the two centers, *S*<sub>μν</sub> is the overlap integral between two basis functions φ<sub>μ</sub> and φ<sub>ν</sub> on the N and O atoms, respectively, and *P*<sub>μν</sub> are the products of their coefficients summed over all occupied spin orbitals. The increase in *P*<sub>NO</sub> confirms the decreasing population

of the NO antibonding orbitals (which give negative contributions to *P*<sub>μν</sub>). The geometric distortion expressed by the basal N(O)–Ru–N angle, which has been interpreted as a measure of trans influence,<sup>29</sup> shows little systematic variation in the series.

The theoretical MS1 – GS energy differences Δ*E* are listed in the last row of Table 3. The *trans*-nicotinamide complex has an MS1 Δ*E* value similar to that of NH<sub>3</sub>, in agreement with the similar decay temperatures of the *trans*-nicotinamide and *trans*-NH<sub>3</sub> [Ru(NH<sub>3</sub>)<sub>4</sub>(NO)] complexes.

### Concluding Remarks

While the redox potentials and the NO-stretching frequencies can be used as rough indications for the relative stability of the isonitrosyl-linkage isomers, the results on the [Ru(NH<sub>3</sub>)<sub>4</sub>(NO)-nic] salts show that such a correlation has only approximate predictive power. Thus, the identification of a single physical indicator for linkage isomer stability remains elusive.

On thermal decay of the isonitrosyl state, the complex passes through the intermediate MS2 geometry.<sup>4</sup> As the MS2 state is not observed in the experiments, the barrier for the second step, the MS2 → GS rearrangement, must be relatively low. Thus, the kinetics for the return of the isonitrosyl species to the ground state should be governed by the height of the MS1 → GS transition state barrier. Calculations of the transition state are being undertaken in order to provide further guidelines for the identification of high-*T*<sub>d</sub> linkage isomers.

**Acknowledgment.** Support of this work by the National Science Foundation (CHE9981864, P.C.; MCB9723828, K.A.B.) and the Petroleum Research Fund, administered by the American Chemical Society (PRF28664AC3, P.C.), is gratefully acknowledged. Theoretical calculations were carried out on the SGI Origin-2000 supercomputer at the Center for Computational Research at SUNY/Buffalo, which is supported by a grant (DBI9871132) from the National Science Foundation.

**Supporting Information Available:** Atomic coordinates, anisotropic and hydrogen isotropic displacement parameters, bond lengths and angles for [Ru(NH<sub>3</sub>)<sub>4</sub>(NO)nicotinamide]<sup>3+</sup>, in CIF format. This material is available free of charge via the Internet at <http://pubs.acs.org>.

IC000583D

(29) Lyne, P. D.; Mingos, D. M. P. *J. Chem. Soc., Dalton Trans.* **1995**, 1635–1643.